Technical Journal, University of Engineering and Technology (UET) Taxila, Pakistan Vol. 28 No. 2-2023
ISSN:1813-1786 (Print) 2313-7770 (Online)

Rock Physics Modelling of Sub-Seismic Reservoirs In Complex Depositional Systems: Case Study of Sand_K2, 'Kuti' Field, Deepwater Niger Delta, Nigeria

S. Oladele[1], R. Salami[2], J. R. Onayemi[3]

[1,2,3]*University of Lagos, University Road Lagos Mainland Akoka, Yaba, Lagos, Nigeria*

[1] soladele@unilag.edu.ng

Abstract- Sand_K2 is a thin, sub-seismic reservoir in 'KUTI' Field, Deepwater Niger Delta having indistinct impedance contrast with the surrounding shale wish made conventional seismic interpretation impossible. Rock physics transformation of petrophysical properties of Sand_K2 into petro-elastic parameters, which allows sub-seismic reservoir to be imaged from seismic data, has been carried out. The reservoir's lithofacies and their petrophysical properties were determined using well data. Rock physics analysis was implemented to model the seismic response of the reservoir. The rock physics analysis was achieved through multivariate cross-plot of petro-elastic parameters of the Sand_K2. Sand_K2 has a thickness of 32.8m, shale volume of 12%, average porosity of 33% and acoustic impedance of 4200 to 5000 (m/s)(g/cc). The presence of shale and clay minerals increases the acoustic impedance and P-wave velocity of the reservoir above 4800 (m/s)(g/cc) and 2500 m/s respectively; while decreasing its porosity and rigidity (Mu-Rho) below 36% and 6.0 (Gpa*g/cc) respectively. The effect of hydrocarbon reduced acoustic impedance below 4775 (m/s)(g/cc). Similarly, the hydrocarbon effect reduced the reservoir's incompressibility (Lambda-Rho) below 25 (Gpa*g/cc). Rock physics modelling provided calibration data from which cut-off values were determined for improved identification and interpretation of sub-seismic reservoirs awayfrom the wellbore, consequently reducing exploration risks.

Keywords- Rock Physics, Cross-Plot, Petro-Elastic, Sub-Seismic, Lambda-Rho

I. INTRODUCTION

Hydrocarbon exploration in the Gulf of Guinea is progressively moving into geologically more complex ultra-deep offshore as onshore/shallow offshore deposits are rapidly depleted. In general, the deepwater setting is mostly regarded as a prolific hydrocarbon province all over the world with significantly huge distributions of stratigraphic traps, but the least understood geological environment due to its complexity [1-2]. Consequently, in most deepwater systems, such as the turbidite systems, more than 70% of the mobile oil is commonly left behind, because of the complex nature of these reservoirs [3-4]. Deepwater Niger Delta is very prolific but characterized by a complex geologic setting usually typified by reservoirs that are generally thin, vertically stacked and laterally discontinuous with indistinct impedance contrast with the surrounding shale [5-7]. These complexities have made regular seismic interpretation becomes increasingly ambiguous and uncertain, making the task of finding hydrocarbon herculean, thus causing huge capital losses in the petroleum industry as noted by [8-11].

The theory and principle of rock physics have been discussed in detail by [12-14]. According to several authors [15-21] who have employed the tool of rock physics modelling; one of the panaceas to reduce uncertainty and improve the chances of success of seismic exploration in such geologically complex settings is the linkage of rock physics properties to their corresponding seismic responses. The application of rock physics tools will provide an enhanced understanding of the true geologic meaning of seismic amplitudes in such areas. Rock physics permits modelling and quantification of the seismic output of reservoir properties recorded in Wells, thus providing datasets that are comparable with observed seismic. Rock physics employs the output of petrophysical evaluation as input in addition to the results of laboratory measurements, where available, and combines these using theoretical and empirical

relations to understand how seismic signal responds to changes in the reservoir properties [22]. According to [23] "all exploration is ultimately related back to rock properties and the only way to connect rock properties to seismic amplitude or response is to use rock physics". In this study, a dataset from KUTI Field located about 120 km southwest offshore Niger Delta and at a water depth of 1000m in the translational zone of the Western Lobe (Fig. 1) was utilized. The reservoirs are unconsolidated turbidite sandstones of the offshore paralic sequence. Preliminary analysis of the available dataset revealed two major problems that are associated with the study area which pose a great challenge to conventional seismic interpretation workflow. Firstly, the reservoirs are generally prolific, vertically stacked but thin (the thickest being 32.8m in this study) and fall below seismic resolution (tuning thickness of 36.2m). Secondly, there is a very poor impedance contrast between the sands and the surrounding shale. These conditions made it practically impossible to image the reservoirs from conventional seismic interpretation; a possible reason why most of the Wells drilled earlier in the study area were suspended despite significant oil and gas shows. None of the reservoirs are resolved on the seismic data as the top and base of each reservoir occur within a single wavelet lobe on the synthetic trace. Also, the wavelet that defines each reservoir also extends to the overlying seal (shale), indicating poor impedance contrast between the sand and the surrounding shale.

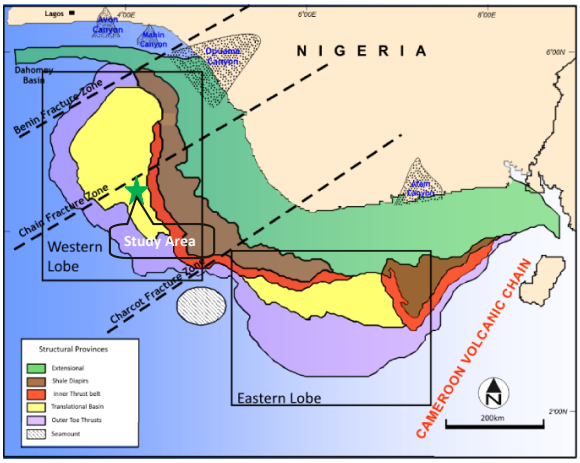

Figure 1: Map of Niger Delta showing the study area and five structural provinces (After [24])

II. Geological Framework

The geological framework of the Niger Delta has been widely researched by numerous workers such as [25-30]. Generally, the stratigraphy of the Niger Delta is characterized by three broad lithologies; Akata Formation, Agbada Formation and Benin Formation (Fig. 2). The Akata Formation is mainly over-pressured and under-compacted marine shale, which forms the base of the known deltaic sequence and extends across all depo-belts. Akata Formation was deposited in the Holocene and represents the major source in the Niger Delta. The Agbada Formation is essentially a paralic sequence of shale, silt and sand which succeeded the underlying Akata Formation. It was deposited from Eocene to Pleistocene and hosts the reservoir and sealing facies which spread in varying proportions across all depo-belts. The continental Benin Formation is the shallowest part of the sequence, which was deposited during the Oligocene. It thins out offshore and disappears completely near the shelf edge. The offshore and deepwater section of the Niger Delta evolved from continuous progradation of the delta and seaward movement of the monotonous marine shale. The paralic sequence in this section was formed in the Late Miocene as documented by [31].

III. Materials and Methods

This study utilized subsurface data from four Wells (KUTI-01, KUTI-02, KUTI-03, and KUTI-04), Check-shot data and a fully stack Time Migrated 3D Seismic data. The properties of the seismic data are summarized in Fig. 3. In general, the Well logs were of good quality. The data were acquired, processed and made available by Shell Nigeria. Hampson Russell software was employed for data visualization and interpretation.

Petrophysics Analysis of Sand_K2

Gamma-ray, neutron and density logs were combined to define the sedimentary facies on the basis of the sand shale ratio. Gamma ray readings of 26 to 30 API were taken as clean sand, and readings of 40 to 70 API were reckoned as shaly sand. Values 80 to 110 API were taken as sandy shale while readings from 110 to 130 were taken as pure shale. Using resistivity logs, the reservoirs were identified and their petrophysical properties determined. Elastic logs such as acoustic impedance (AI), shear impedance (SI), velocity ratios (Vp/Vs), Mu-Rho and Lambda-Rho were computed from the logs and conditioned for rock physics modelling.

Well-Based Rock Physics Analysis

Cluster analysis of AI vs SI vs Gamma Ray was used to discriminate the reservoir from the surrounding shale and to predict the distinctive seismic character of the selected reservoir (SAND_K2) in terms of acoustic impedance and shear impedance.

Subsequent cross-plot analysis was carried out to model variation of seismic character within the selected reservoir in relation to mineralogy, porosity and pore-fluid. The effect of mineralogy was modelled from cross-plots of AI vs. SI vs. Gamma Ray, P-wave velocity vs. Porosity vs. Gamma Ray, and Mu-Rho vs. Lambda-Rho vs. Water Saturation. The effect of porosity was modelled from a multivariate cross-plot of P-wave velocity vs. Porosity vs. Gamma Ray. The effect of pore-fluids was modelled from cross-plots of Vp/Vs vs. AI vs. Water Saturation and Mu-Rho vs. Lambda-Rho vs. Water Saturation. Results of multivariate cross-plot were displayed in the form of rock physics templates showing the link between reservoir parameters and their seismic response.

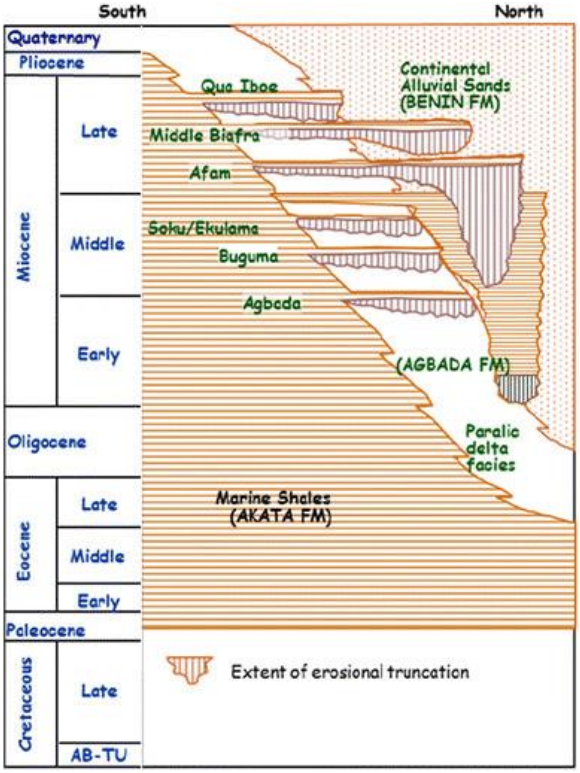

Figure 2. Regional stratigraphy of the Niger Delta showing different Formations [32]

Quantitative Seismic Analysis

Using the outputs of Well-based rock physics analysis, the seismic response of SAND_K2 was computed for each modelled parameter, from which cut-off values of amplitudes were determined in terms of AI, P-wave velocity, lambda-Rho and porosity. The cut-off values provided a set of data that aids the identification and discrimination of the reservoir at the well location and predicts the most plausible lateral distribution of the reservoir and the fluid contents away from the well location using seismic data.

SEISMIC DATA – KUTI_Vol	
Field Type	Deep Offshore (Water depth of 100m)
Data Type	3D Post-Stack Time Migrated (PSTM)
Gather Type	Common Depth Point (CDP)
Polarity	Normal Polarity
Wavelet	Minimum Phase
Dominant Freq	20 Hertz
Tuning Thickness	36.2m
In-lines	1207 (669494 - 670701)
Cross-lines	885 (493777 - 494662)

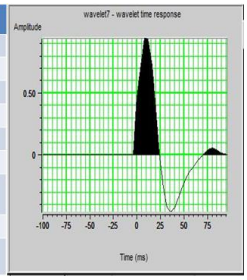

Figure 3: Summary of properties of the seismic data used for the study and the extracted wavelet.

IV. Results and Discussion

Reservoir Identification and Lithostratigraphic Framework

The result the of Seismic-to-well tie at the location of Well KUTI-01(Fig. 4) shows a good character tie (87% correlation). The reservoirs are generally vertically stacked but thin and fall below seismic resolution. Furthermore, there's a very poor impedance contrast between the sands and the surrounding shale. These conditions will make it practically impossible to image these reservoirs from conventional seismic interpretation. Also, the wavelet that defines each reservoir also extends to the overlying seal (shale), indicating poor impedance contrast between the sand and the surrounding shale.

The one-dimensional lithofacies framework (Fig. 5a) reveals the various lithofacies penetrated by Well KUTI-01. The entire column shows a general coarsening-up sequence (progressive decrease in gamma ray) from the base of the Well upwards as indicated by the arrows. This reflects a characteristic mud-dominated submarine fan system with a sand-shale ratio increasing from the lower mud-dominated section to the upper sandy section. The trapped sands (K1–K4) within this system provide stacked reservoirs which are penetrated by the Well (Fig. 5b). These reservoirs facies show fining-up patterns (increasing gamma ray), reflecting characteristic submarine channel deposits (Fig. 5a). SAND_K2, representing the most promising prospect, was selected as the target reservoir. The result of the petrophysical evaluation of SAND_K2 is summarized in Fig. 5c.

Elastic Characteristics of Sand_K2

Fig. 6 is the rock physics template derived from the cross-plot of AI vs SI colour-coded with gamma-ray along the interval of the target reservoir and the overlying shale. Two distinct clusters were observed in response to the impedance contrast between the

reservoir and the surrounding shale. The clusters have been interpreted as reservoir SAND_K2 and shale (sealing rock) based on the gamma-ray colour code. The reservoir has an acoustic impedance range of 4400 to 5200 (ms)*(g/cc) and a shear impedance of 1100 and 1350 (ms)*(g/cc). On the other hand, the shale has an acoustic impedance range of 6800 to 7400 (ms)*(g/cc) and a shear impedance range of 1600 to 1900 (ms)*(g/cc). The shale trend is in the direction of increasing acoustic and shear impedance.

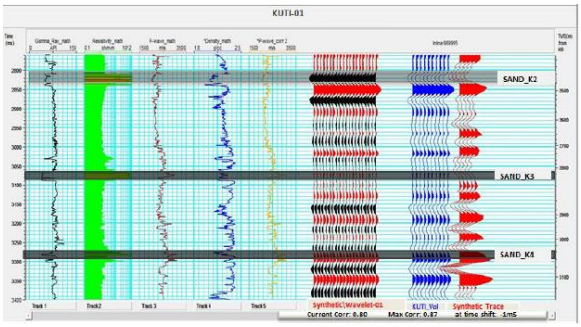

Figure 4: Seismic-to-Well Tie at location of Well KUTI-01 with a good character tie of 87%

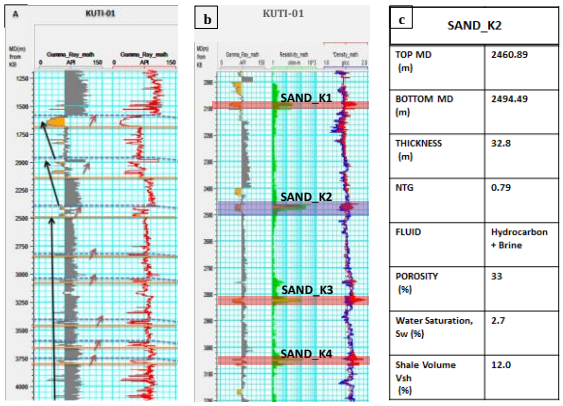

Figure 5: (a) One-dimensional Facies Model of Well KUTI-01 showing the various lithofacies penetrated by the Well; (b) shows the various reservoir facies that exist within the column; and (c) shows result of the petrophysical evaluation of target reservoir (SAND_K2).

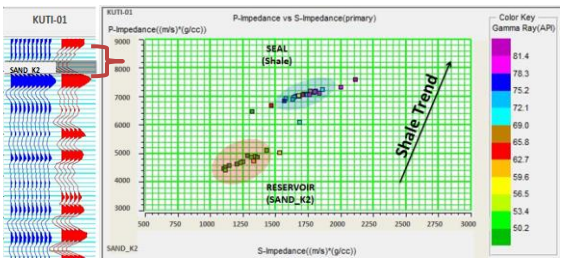

Figure 6: Well-based Rock Physics Template from cross-plot of AI vs. SI colour-coded with gamma ray log along the interval of SAND_K2 and overlying seal in Well KUTI-01. Good discrimination between lithologies and strong impedance contrast between the reservoir and seal.

Effect of Clay Content and Porosity on Seismic Characteristics of Reservoir

Effect of mineralogy on the seismic response of SAND_K2 is represented in Fig. 7. The multivariate cross-plot of AI vs SI colour-coded with gamma-ray (Fig. 7) produces two clusters in response to mineralogical heterogeneity within the reservoir. Based on the gamma-ray colour code, the clusters have been interpreted as the clean zone and the shaly zone. The clean zone has an AI range from 4000 to 4800 (ms)*(g/cc), and an SI range from 1100 to 1500 (ms)*(g/cc). The presence of shale increases the acoustic impedance and shear impedance slightly above 4800 (ms)*(g/cc) and 1500 (ms)*(g/cc) respectively. Owing to the higher density of shale and the direct relationship between impedance and density, the shaly zone has a higher impedance than the clean zone.

Cross-plot of P-wave velocity vs Porosity colour-coded with gamma-ray (Fig. 8) reveals the effect of pore spaces and mineralogy on the seismic signature of SAND_K2. Three distinct clusters are identified in response to porosity and mineralogical variations within the reservoir. The clusters have been interpreted as clean sand, shaly sand and sandy shale based on the gamma-ray colour code. The clean sand has the highest average porosity of 36% and the lowest P-wave velocity range of 2000 to 2400 m/s. The presence of clay minerals decreases reservoir porosity below 36% and down to 26% (sandy shale) while increasing the P-wave velocity above 2400 m/s and up to 3000 m/s (sandy shale). In general, the presence of clay minerals in a clastic reservoir rock is likely to clog up pore spaces within and reduce sorting, thereby decreasing its effective porosity. As pore spaces are clogged up, the minerals become closer to one another due to cementation, thereby increasing the seismic P-wave velocity of the reservoir. Consequently, an increase in clay minerals reduces the average porosity and increases P-wave velocity (Fig. 8).

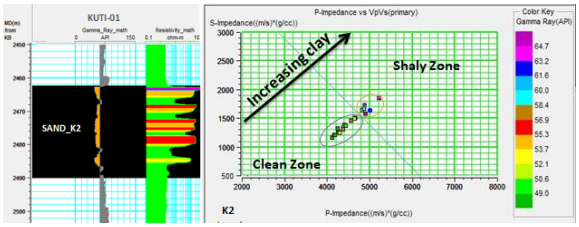

Figure 7: Well-based Rock Physics Template from cross-plot of AI vs.SI colour-coded with gamma ray along the interval of SAND_K2 in Well KUTI-01,

showing variation of impedance within the reservoir in response to mineralogical heterogeneity.

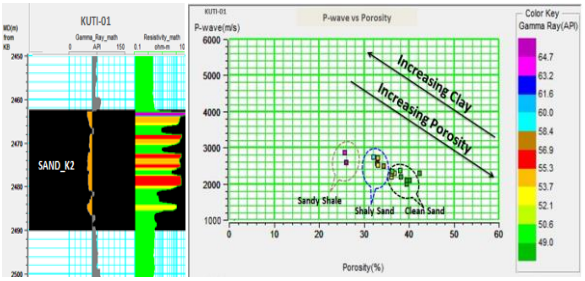

Figure 8: Well-based Rock Physics Templates from cross-plot of P-wave velocity vs. Porosity colour coded with Gamma ray for SAND_K2 in Well KUTI-01, showing the variation of seismic P-wave velocity within the reservoir in response to change in mineralogy and porosity.

Contribution of Pore-Fluid and Mineralogy on Seismic Response of SAND_K2

The contribution of pore-fluid and mineralogy on the seismic response of SAND_K2 is represented by the template in Fig. 9. Cross-plot of Mu-Rho vs Lambda-Rho colour coded with water saturation (Fig. 9) reveals changes in the reservoir's rigidity and incompressibility respectively, in response to fluid and mineralogical variability. Lambda is an elastic property of rock known as incompressibility, derived from seismic P-wave. It responds primarily to the type of fluids filling the pore spaces. Denser fluid like brine increases incompressibility, while hydrocarbon reduces incompressibility with gas having the most reducing effect. Therefore, the product of Lambda and density (Lambda-Rho) gives good discrimination between different pore fluids. On the other hand, Mu is an elastic parameter of rocks known as rigidity, derived from seismic shear waves. It is a measure of resistance exerted by the rock matrix to shearing. Therefore, it responds primarily to mineralogy. The value is usually higher in the sand because sand particles offer more resistance to shearing than shale. The product of rigidity (Mu) and density (Mu-Rho) provides good discrimination between sand and shale. In Figure 9, the clean (sandy) zone is towards the quartz line with higher values of Mu-Rho, indicating high rigidity. Meanwhile, the shaly zone is towards the shale line with lower values of Mu-Rho, indicating lower rigidity. The shaly zone contains mostly brine, and has a higher average value of Lambda-Rho (about 26.1 (GPa*g/cc)), indicating higher incompressibility. The clean (sandy) zone contains mostly hydrocarbon, and a lower average value of Lambda-Rho (about 23.9 (GPa*g/cc)), indicating lower incompressibility. The presence of hydrocarbon reduces the incompressibility of the reservoir below the Lambda-Rho value of 25(GPa*g/cc), with gas (A) causing a reduction further below 24 (GPa*g/cc).

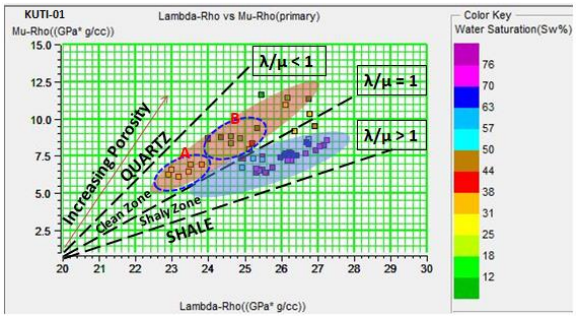

Figure 9: Well-based Rock Physics Template from cross-plot of Mu-Rho vs Lambda-Rho colour coded Water Saturation for SAND_K2 in Well KUTI-01, showing changes in the reservoir rigidity and incompressibility in response to fluids and mineralogical variability: A – gas filled pores; B – oil filled pores.

Modelling of Seismic Response to Pore Fluids

The response of different pore fluids on the seismic signal of the reservoir is symbolized by the template in Fig. 10. Multivariate cross-plot of velocity ratios vs AI, colour coded with water saturation (Fig. 10) reveals variation in the acoustic impedance within Sand_K2 in response to fluid heterogeneity in the pore spaces. Two distinct clusters are evident which have been interpreted as hydrocarbon-fill pores and brine+ hydrocarbon-fill pores based on the water saturation colour code. The hydrocarbon-fill pores produced an acoustic impedance response between 4100 and 4700 (ms)*(g/cc). The mixed fluid pores created an acoustic impedance response above 4700 (ms)*(g/cc). Because brine is generally denser than hydrocarbon and impedance is directly related to density, the presence of brine in the mixed fluid pores causes these pores to have higher acoustic impedance. The effect of pore-fluids on velocity ratios is quantitatively negligible (less than 0.0001). Qualitatively, however, the hydrocarbon-fill pores have slightly higher values of velocity ratios than the mixed fluid pores (Fig. 10). Conventionally, brine pores tend to have higher velocity ratios than hydrocarbon pores owing to higher P-wave value. However, the presence of a significant volume of hydrocarbon (most likely dissolved gas) in the mixed fluid zone must have reduced the incompressibility of the rock matrix, and hence the seismic P-wave velocities, resulting in slightly lower values of velocity ratios. Similar results were obtained from a seismic-based cross-plot of velocity ratios vs.

acoustic impedance using seismic amplitudes extracted from model-based inversion (Fig. 11). The hydrocarbon-fill pores have slightly higher velocity ratios, but lower AI than the mixed fluid pores. Also within the hydrocarbon-fill pores, two distinct clusters are produced in response to different hydrocarbon types; oil (B), which has higher acoustic impedance than gas (A) owing to its density.

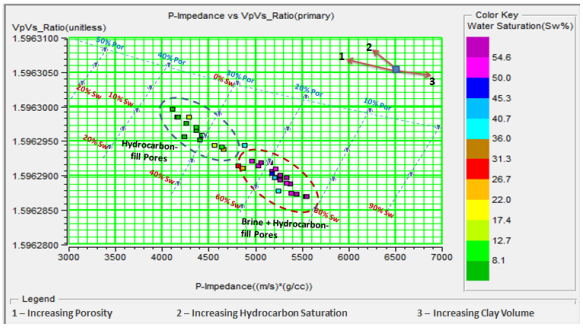

Figure 10: Well-based Rock Physics Template from cross-plot of Vp/Vs vs. AI colour coded with Water Saturation for SAND_K2 in Well KUTI-01, showing the variation of acoustic impedance within the reservoir in response to different pore fluids.

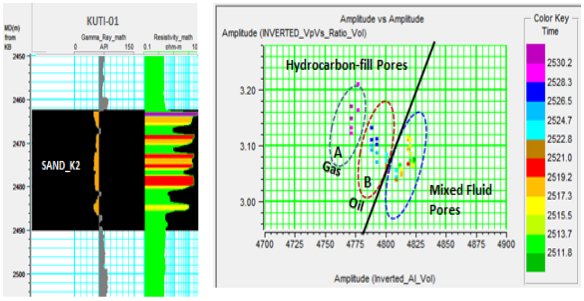

Figure 11: Seismic-based Rock Physics Template from cross-plot of V_p/V_s ratios amplitude vs AI amplitude for SAND_K2 within the location of Well KUTI-01, showing the variation of acoustic impedance within the reservoir in response to different pore fluids.

Elastic Properties and Seismic Response of Sand_K2

Results of the quantitative rock physics analysis of Sand_K2 are summarized in Tables I and II. Table 1a represents the elastic properties of the reservoir relative to the surrounding shales in terms of acoustic impedance and shear impedance. Table II represents the seismic response of the reservoir due to mineralogy, porosity and pore fluids. Rock physics modelling, using available logs and petrophysical evaluation has helped in better understanding sub seismic reservoir, and allows further interpretation of the lateral distribution of the reservoir possible using seismic amplitude information.

Table I: ELASTIC PROPERTIES OF SAND_K2 RELATIVE TO THE SURROUNDING SHALE

Acoustic Impedance(ms)*(g/cc) **Reservoir Sand/ Shale/ Cut-off Value**	**Shear Impedance(ms)*(g/cc)** **Reservoir Sand/ Shale/ Cut-off Value**
4200 – 5000 Above 5000 5000	1100 – 1500 Above 1500 1500

Table II: SEISMIC RESPONSE OF SAND_K2

AI(ms)*(g/cc) **Clean Sand/ Shaly-Sand/ Cut-off Value**	**SI(ms)*(g/cc)** **Clean Sand/ Shaly-Sand/ Cut-off Value**	**P-wave (m/s) Clean Sand/ Shaly-Sand/ Cut-off Value**	**Porosity (%) Clean Sand/ Shaly-Sand/ Cut-off Value**	**Lambda-Rho (GP*g/cc) Gas/ Oil/ Brine/ Hydrocarbon -Brine Cut-off**
4000 – 4800 Above 4800 4800	1100 – 1500 Above 1500 1500	2000 – 2400 Above 2400 2400	32 – 40 23 – 30 30	23 – 24 24 – 25 Above 25

V. Conclusion

The target reservoir (SAND_K2) is a channel sand of a mud-dominated submarine fan system penetrated. SAND_K2 has thickness of 32.8m with shale volume of 12%, average porosity of 33% and hydrocarbon saturation of 97.3%. The P-wave velocity, rigidity (Mu-Rho), acoustic and shear impedance provided good lithologic discrimination between SAND_K2 and the surrounding shale.

Lambda-Rho amplitude differentiated between hydrocarbon-fill pores and brine-fill pores while the seismic amplitude further segregated the gas and oil within the hydrocarbon-fill pores; The study has shown that well log derived Rock physics attributes (integrated with seismic characters), can assist in improved identification, discrimination and interpretation of sub seismic reservoirs and allow prediction of the lateral distribution of such reservoirs away from wellbore, consequently reducing exploration risks.

VI. Acknowledgement

The authors thank Shell E & P Company in Nigeria for making the dataset available for this study.

References

[1] Stevenson, R. J., Zalack, J. T., & Wolin, J. (2013). A multimetric index of Lake Diatom condition based on surface-sediment assemblages. *Freshwater Science*, 32, 1005–1025. https://doi.org/10.1899/12-183.1.

[2] Celik, H. (2013).The effects of linear coarse grained slope channel bodies on the orientations of fold developments: A case study from middle Eocene-Lower Oligocene Kirkgecit Formation Elazig. eastern Turkey. *Turkish Journal of Earth Sciences.* 2013. 22. pp. 320- 338

[3] Pettingill. H. S .. and Weimer. P. (2002). Global Deep Water Exploration: Past. Present and Future Frontiers: *The Leading Edge.* 21. 371-376.

[4] Avseth. P .. Mukerji. T .. and Mavko. G. (2005). Quantitative Seismic Interpretation: Applying Rock Physics Tools to Reduce Interpretation Risk. Cambridge Univ ersity Press. New York. NY. 408pp.

[5] Oladele, S .. Salami. R .. and Adeyerni, B. (2019). Petrophysical and Rockphysics Analyses for Characterization of Complex Sands in Deepwater Niger Delta. Nigeria: *GeoScience Engineering.* Volume LXV (2019). No.2 p. 24 - 35. DOl 10.35180/gse-2019-0009.

[6] Caers, J. Avseth P. and Mukerji T. (2001). Geostatistical integration of rock physics. Seismic amplitudes and geologic models in North Sea turbidite systems: The *Leading Edge. 308*-312.

[7] Wood. J. Lesli, Daniel Pecuch and Ben Schulein. (2000). Seismic attribute and sequence stratigraphic integration methods for resolving reservoir geometry in San Jorge Basin. Argentina: *The Leading Edge. 95*

[8] Tyler, N. and Finley. R. J. (1991). Architectural controls on the recovery of hydrocarbon from sandstone reservoirs. In Three-Dimensional Facies Architecture of Terrigerlous Clastic Sediment sand its Implications for Hydrocarbon Discovery and Recovery (ed. Miall, A. D. and Tyler. N}.Tulsa: Society of Sedimentary Geologists. 1-5.

[9] Lawrence, D. T. and Bosman-Smits. D. F. (2000). Exploring deep water technicalchallenges in the Gulf of Mexico. *In* P. Weimer. R. M. Slatt, J. L. Coleman .. Rosen, C. H.Nelson, A. H. Bouma. M. Styzen, and D. T. Lawrence, cds .2000. Global Deepwater Reservoirs: Gulf Coast Section *SEPM Foundation* Bob F. Perkins 20th Annual Research Conference. 473-477.

[10] Bakke. k .. Kane. LA .. Martinsen. O. 1.. Petersen. S. A .. Johanson. T. A.. Huston: S .. Jacobson. F. H.. and Groth A. (2013). Seismic modeling in the analysis of deepwater sandstone termination *style. AAPG* Bulletin. 97 (9).1395-1419.

[11] Okeugo, C. G., Onuoha, K.M .. Ekwe, C.A .. and Dim. C.l.P. (20I8). Application of crossplot and prestack seismic-based impedance inversion for discrimination of lithofacies and fluid prediction in an old producing field. Eastern Niger Delta Basin.

[12] Avseth. P .. Mukerji. T .. and Mavko. G. (2005). Quantitative Seismic Interpretation: Applying Rock Physics Tools to Reduce Interpretation Risk. Cambridge Univ ersity Press. New York. NY. 408pp.

[13] Avseth, P .. Mukerji. Too Mavko. G .. and Tyssekvam. J. A. (2001). Rock Physics and AVO Analysis for Lithofacies and Pore Fluid Prediction in a North Sea Oil Field.The Leading Edge. 20. 429.

[14] Avseth. P .. Dvorkin. l..Mavko. G. and Rykkje. J. (2000). Rock physics diagnostic of North Sea sands: Link between microstructure and seismic properties. Geophysics Research Letters, vo1.27. Iss.17. p.2761-2764. doi: 10.1 029/1999GL008468

[15] Avseth. P. Johansen T. A.. AimanBakhorji and Husam M. Mustafa (2014). Rock-physics Modelling Guided by Deposition and Burial History in Low-to-intermediate-porosity Sandstones. Geophysics. vol. 79. NO.2, P. 0115-0121.10.1190/GE02013-0226.1

[16] Razaq, B., Igwenagu, C. Linda and Onifade, Y. S. (2015): "Cross plotting of Rock Properties for Fluid and Lithology Discrimination using Well Data in a Niger Delta Oil Field." Journal of Applied Science and Environmental Management. Vol. 19 (3) 539 - 546.

[17] Kabanda A (2017) Rock physics template (RTP) technology for reservoir characterization and 4D seismic monitoring. CSEG Recoder 42(1):30–33.

[18] Horsfall. O. L E.D. Uko. I. Tamunoberetonari, and V. B. Omubo-Pepple. (2017). Rock-Physics and Seismic-Inversion Based Reservoir Characterization of AKOS FIELD. Coastal Swamp Depobelt, Niger Delta. Nigeria: IOSR Journal of Applied Geology and Geophysics (IOSR-JAGG). e-ISSN: 2321 0990. p-ISSN: 2321-0982.Volume 5. Issue 4 Ver. III. PP 59-67

[19] Adeoti, L.. Alo. O. J .. Ayolabi. E. A .. Akinmosin, A.. Oladele. S .. Oyeniran, T .. and Ayuk. M. A. (2018). Reservoir Fluid Determination from Angle Stacked Seismic Volumes in 'Jay' Field. Niger Delta. Nigeria. Journal of Applied Science and Environmental

Management. Vol. 22 (4) 453 - 458 April 2018.

[20] Ogbamikhumi, A and Igbinigie. N. S. (2020). Rock Physics Attribute Analysis for Hydrocarbon Prospectivity in Eva Field Onshore Niger Delta Basin. Journal of Petroleum Exploration and Production Technology 14 (3).

[21] Akinyemi. O. D .. Ayuk. M. A. (2022). Rock physics analysis as a tool for enhancing characterization of Niger Delta deep water sands. *Arab .J Geosci* 15.98 https:lldoi.orgl1 0.1 007 *ls* 12517··021-093 70-8

[22] Hall, J. and Alvarez. E., (2014). Petrophysics for Rock Physics: What Really Matters at Seismic Scale? Paper presented at the SPWLA ss" Annual Logging Symposium. Abu Dhabi, United Arab Emirates.

[23] Corredor. F .. 1. II. Shaw. and J. Suppe. (2005). Shear fault-bend fold. deep-water Niger Delta. in J. H. Shaw. C. Connors.and J. Suppe, eds. Seismic interpretation (if contractional fault related folds: American Association of Petroleum Geologists. A. PG Studies in Geology 53. p. 87-92.

[24] Short, K. C. and Stauble, A. J. (1967). Ouline of geology of Niger delta. American Association of Petroleum Geologists Bulletin. v. 51. p. 761-799.

[25] Merki, P.J. (1971). Structural geology of the Cenozoic Niger delta. In 1st Conference on African Geology Proceedings:Ibadan University Press. p. 635-646.

[26] Weber, K. J. and Daukoru, E. (1975). Petroleum geology of the Niger delta: Tokyo. 9th World Petroleum Congress Proceedings. v. 2. p. 209-221.

[27] Whiteman. A. (1982). Nigeria-its petroleum geology. resources and potential. London, Graham and Trotman. p.394.

[28] Avbovbo. A. A. (1978). Tertiary lithostratigraphy of Niger delta: American Association of Petroleum Geologists Bulletin.v. 62. p. 295-306.

[29] Evamy. B. D., Haremboure, J .. Kamerling, P .. Knaap. W. A.. Molloy. F. A ... and Rowlands. P. H.. 1978. Hydrocarbon habitat of Tertiary Niger delta: American Association of Petroleum Geologists Bulletin. v. 62. p. 1-39.

[30] Doust, Hand Omatsola. E .(1990). Niger Delta. In: J. D. Ed-wards and P. A. Santogrossi, Eds, Divergent/Passive Margin Basins. American Association of Petroleum Geologists Memoir. Vol. 48.1990. pp. 201-238.

[31] Ozumba, B. (2013). Geology of the Niger Delta: An Overview for Geophysics Processors. An SPDC presentation for geologists in Nigeria.

[32] Goodway, W; Chen, T; Downton, J (1997). Improved AVO fluid Detection and Lithology Discrimination Using Lame's Petrophysical Parameters.